Supplementary Information (SI)

Growth pathways of exotic Cu@Au core@shell structures: the key role of misfit strain

El yakout El koraychy,[a] Riccardo Ferrando [b]

[a] Physics Department, University of Genoa, Via Dodecaneso 33, 16146 Genoa, Italy.
E-mail: elkoraychy@fisica.unige.it

[b] Physics Department, University of Genoa, Via Dodecaneso 33, 16146 Genoa, Italy and CNR-IMEM
E-mail: ferrando@fisica.unige.it

In Figure S1, we report the ratio between the gyration radius of minority Cu atoms during the growth process and at the beginning of the simulations. The gyration radius has been calculated with respect to its geometric center during the kinetic growth process. The first and second rows of Figure S1 represent the plot of the gyration radius of the Cu atoms in the case of Type I and Type II simulations, respectively. For each configuration, the data are plotted for the three considered temperatures. The results of Figure S1 show that the gyration radii of Cu atoms have qualitatively the same behaviour for all cases and for different temperatures, i.e. gyration radius increases as Au atoms deposit onto the growing nanostructure with a slight increase when temperature increases, especially at larger sizes. This influence of temperature is not observed in the case of Au on Ih mixed seeds.

Fig. S2 illustrate the number of Cu atoms on the surface during the growth of Au shell on pure Cu and intermixed CuAu cores of different shapes. First row shows the results of Au on Cu cores, whereas the second row represents those for Au on mixed CuAu cores. From the results, we clearly observe that the migration of Cu atoms is somewhat activated in the case of Au on Cu seeds, whereas it is negligeable in the case of Au on CuAu seeds.

In Fig. S3, we show the growth pathway of icosahedral shape from icosahedral copper seed obtained at temperature 400 K with deposition rate of 0.1/ns.

In Figures S4-S6, we represent the final structures obtained when depositing Au atoms on both pure Cu and intermixed CuAu seeds of three different shapes such truncated octahedron (Figure S4), decahedron (Figure S5) and icosahedron (Figure S6). For each seed, we report the results of the five performed simulations at three different temperatures with deposition rate of 1 atom every 10 ns. All the structures are of size up to 1000 atoms.

Figure S7 shows the snapshots of the icosahedral growth pathway starting from truncated octahedral seed. The results are obtained during the growth on pure Cu seed at temperature 500 K. In Figure S7, the structure is shown from two different views at each size. At the first stage of the growth, the Au atoms exchange with some Cu surface atoms of TO seed inducing a composition change of the initial TO seed from pure Cu to intermixed CuAu as shown in non-growing (NG) facets of Figure S7(a). Indeed, this intermixing remains on the surface without transferring to the bulk of TO seed. This tendency towards intermixing makes the structure unstable which leads to the formation/disappearance of defects like stacking faults on the (111) facets of the growing cluster. We believe that this effect disturbs the stability of the formed (100) facets which impedes their growth. Consequently, the formation of structure with large (100) facets as shown in Figure S7(b). When the first Au-rich layer is completely covered the initial TO-shaped (see Figure S7(c)), all the (100)-like facets are stretched into diamond-shaped close-packed facets. At this stage, the transformation is mostly limited to the nanoalloy surface, while the core is only slightly deformed. However, during the formation of the second Au layer on the top of a pyritohedron-405 Cu@Au-rich core@shell as shown in Figure S7(d), the structure transformed to an incomplete Ih of 561 atoms (Figure S7(e)). This transformation occurred at constant number of atoms after the diagonal contraction of all the square faces.

In Fig. S8, we represent the structure of the core at the beginning and at the end of the growth simulations for the exotic shapes presented in Fig. 2 in the main text. The comparison between the initial and final structures confirms that the TO and Dh seeds reconstruct during the growth of Au shell. Whereas the Ih seed did not know any change till the end of the growth.

In Fig. S9 and Fig. S10 we show simulation results for smaller and larger sizes. For small size (Figure S9), we start from an icosahedral of 147 atoms of pure and intermixed compositions and depositing on top of it at a rate of 1 atom/ns to reach size 1000. For large size (Figure S10), we start from a truncated octahedron of 586 atoms of pure and intermixed compositions. From snapshots, we observe that the growth on pure seeds (small and large size) leads to the formation of irregular shapes, however the growth on mixed seeds drives the formation of regular structures.

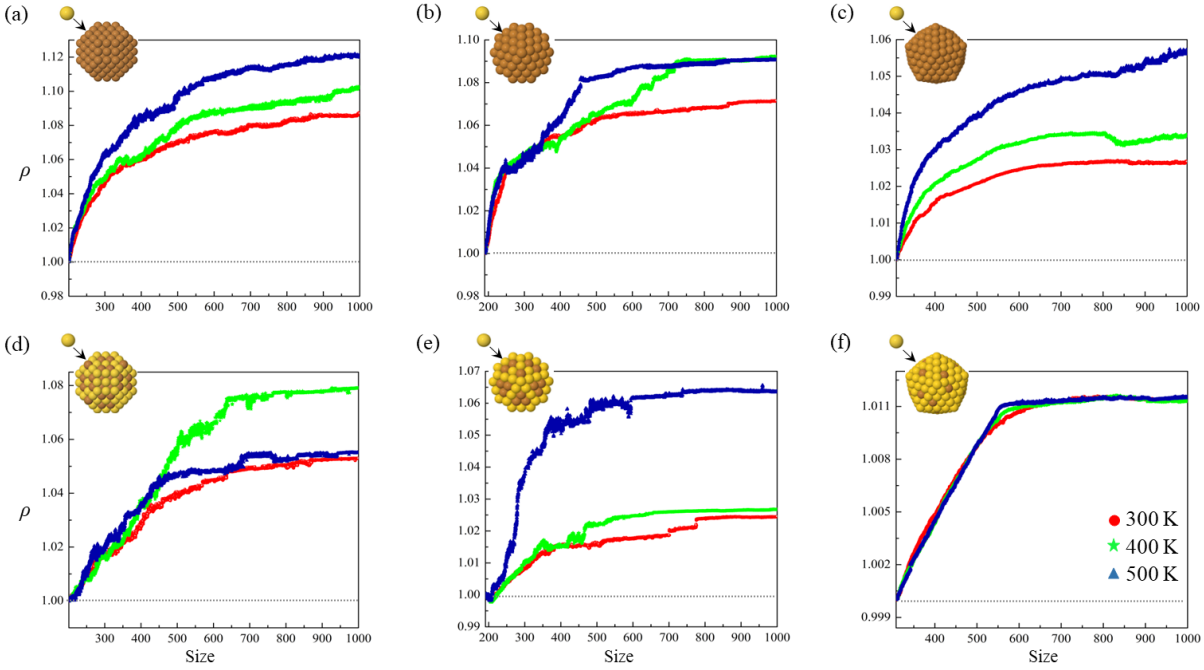

Figure S1: Ratio between gyration radius of Cu atoms at the beginning and during the growth process in the case of type I simulations (first row) and type II simulations (second row). In each graph, red circles, green stars, and blue triangles correspond respectively to temperatures 300, 400 and 500 K.

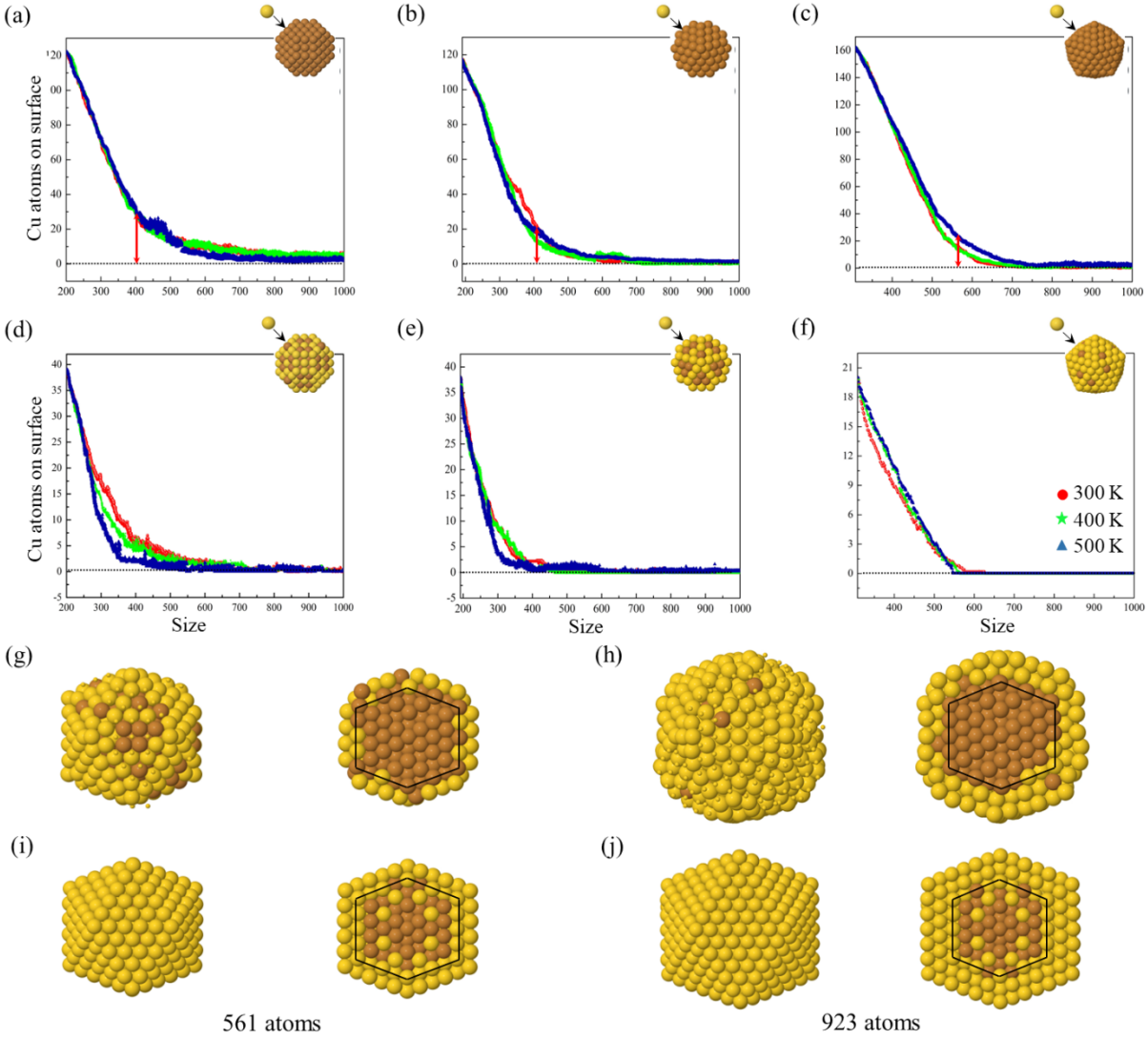

Figure S2: Number of copper atoms in the surface layer during the growth process in the case of type I simulations (first row) and type II simulations (second row). In each graph, red circles, green stars, and blue triangles correspond respectively to temperatures 300, 400 and 500 K. Third and fourth rows represent surface and cross section views of nanoparticles during the deposition of Au atoms on pure and mixed icosahedral seeds, respectively.

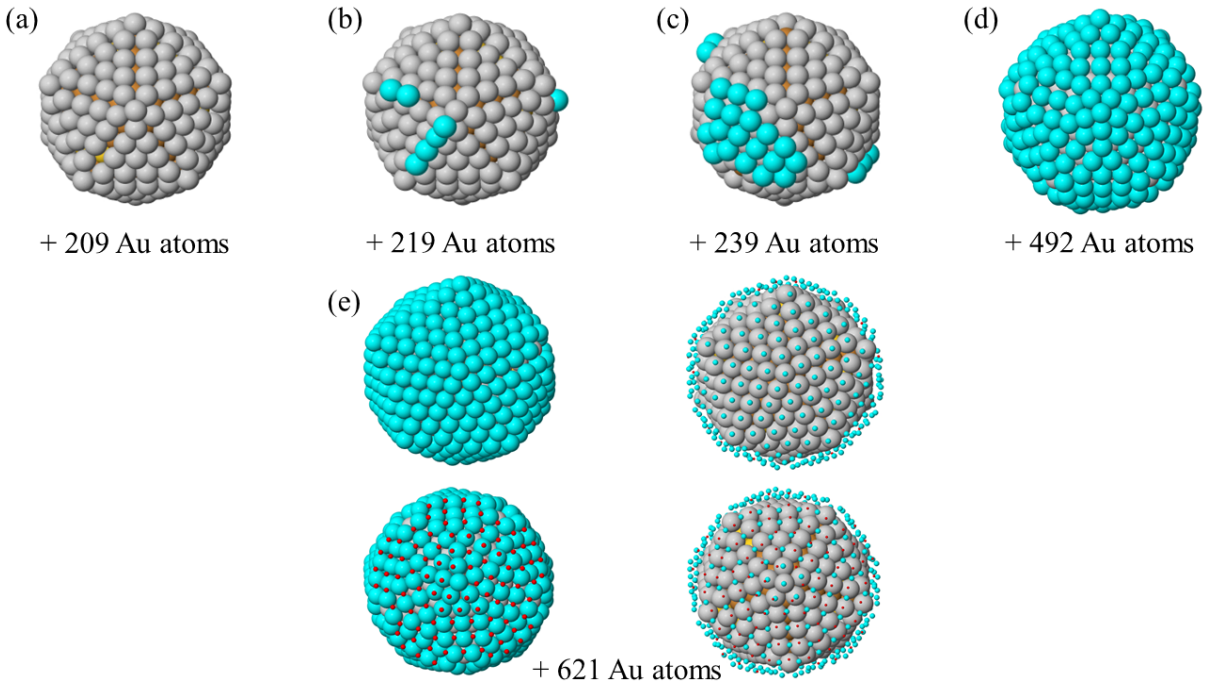

Figure S3: Growth pathway of icosahedral shape from icosahedral copper seed obtained at temperature 400 K with deposition rate of 0.1/ns. For each size, the structure is shown from surface perspective. Gray atoms represent the first formed layer on the initial seed. Cyan atoms show the second formed layer. Red small balls illustrate the third formed layer. (a) a complete anti-Mackay layer formed on the starting icosahedral seed. (b)-(c) nucleation of atoms on the (100) sites of the first anti-Mackay shell. (d) a second anti-Mackay layer on the first one is completely formed. (e) final structure viewed from different sides and shells.

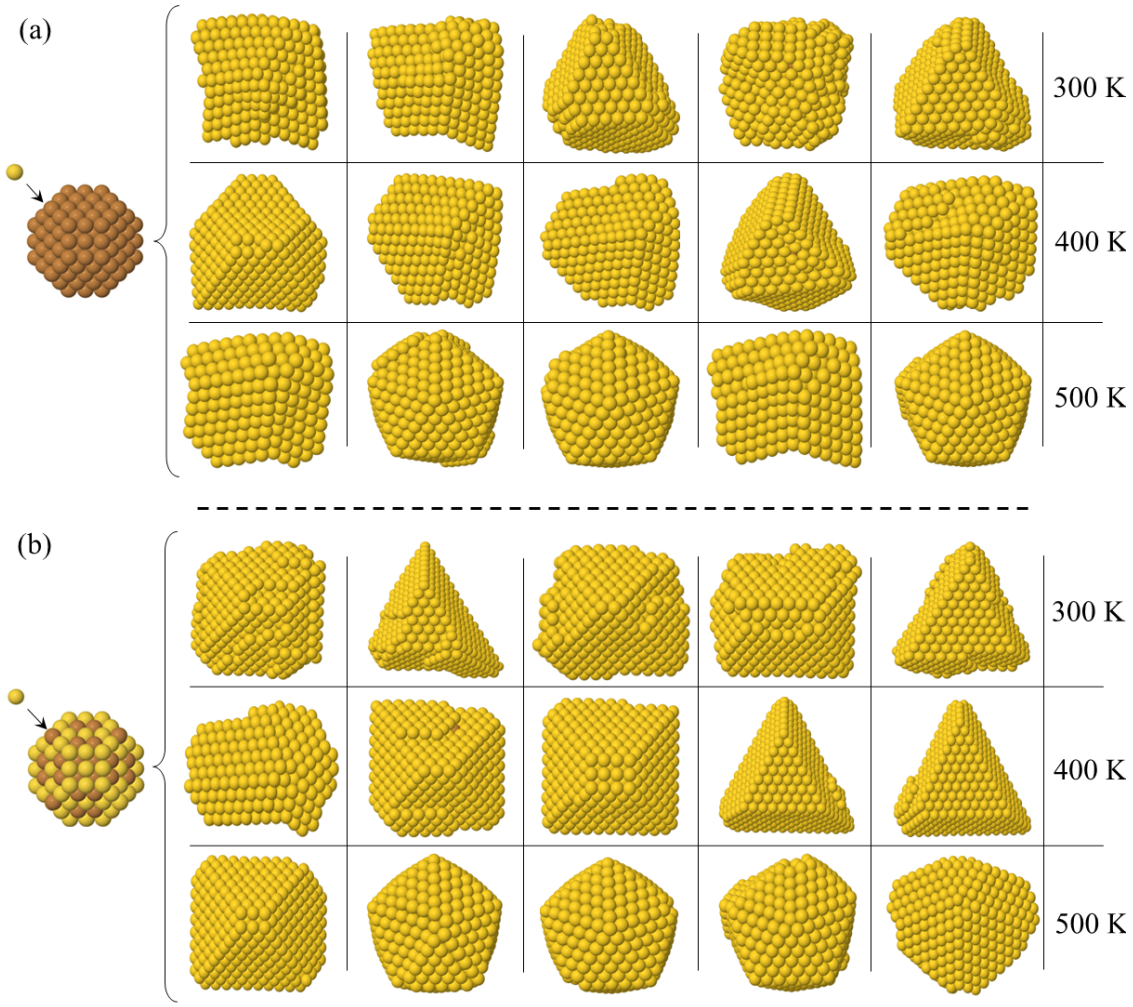

Figure S4: Results of growth on TO seeds with pure Cu (a) and intermixed CuAu (b) compositions obtained at three different temperatures with deposition rate of 0.1 atom/ns. For each seed, the final structures of the five performed simulations are shown. The deposition of Au atoms on Cu TO seed leads to the formation of irregular structures. However, for CuAu TO seed, the growth of common and regular shapes is achieved.

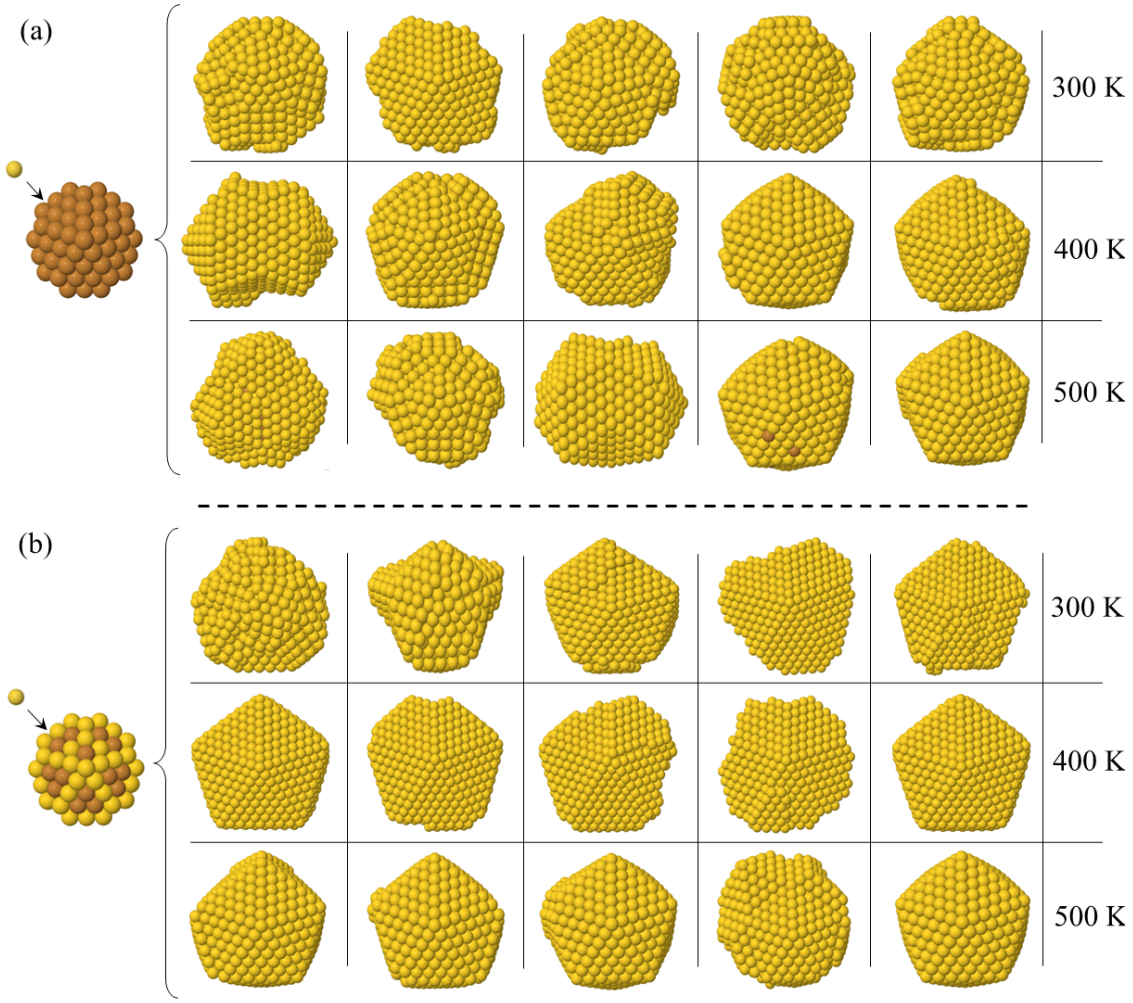

Figure S5: Final structures obtained during the growth of Au atoms on Dh seeds with pure Cu (a) and intermixed CuAu (b) compositions. For each seed and temperature, the results are shown for the five performed simulations with deposition rate of 0.1 atom/ns. In the case of Au on Cu seed, the structures are The deposition of Au atoms on Cu Dh seed leads to the formation of irregular structures. However, for CuAu Dh seed, the growth of common and regular shapes is achieved.

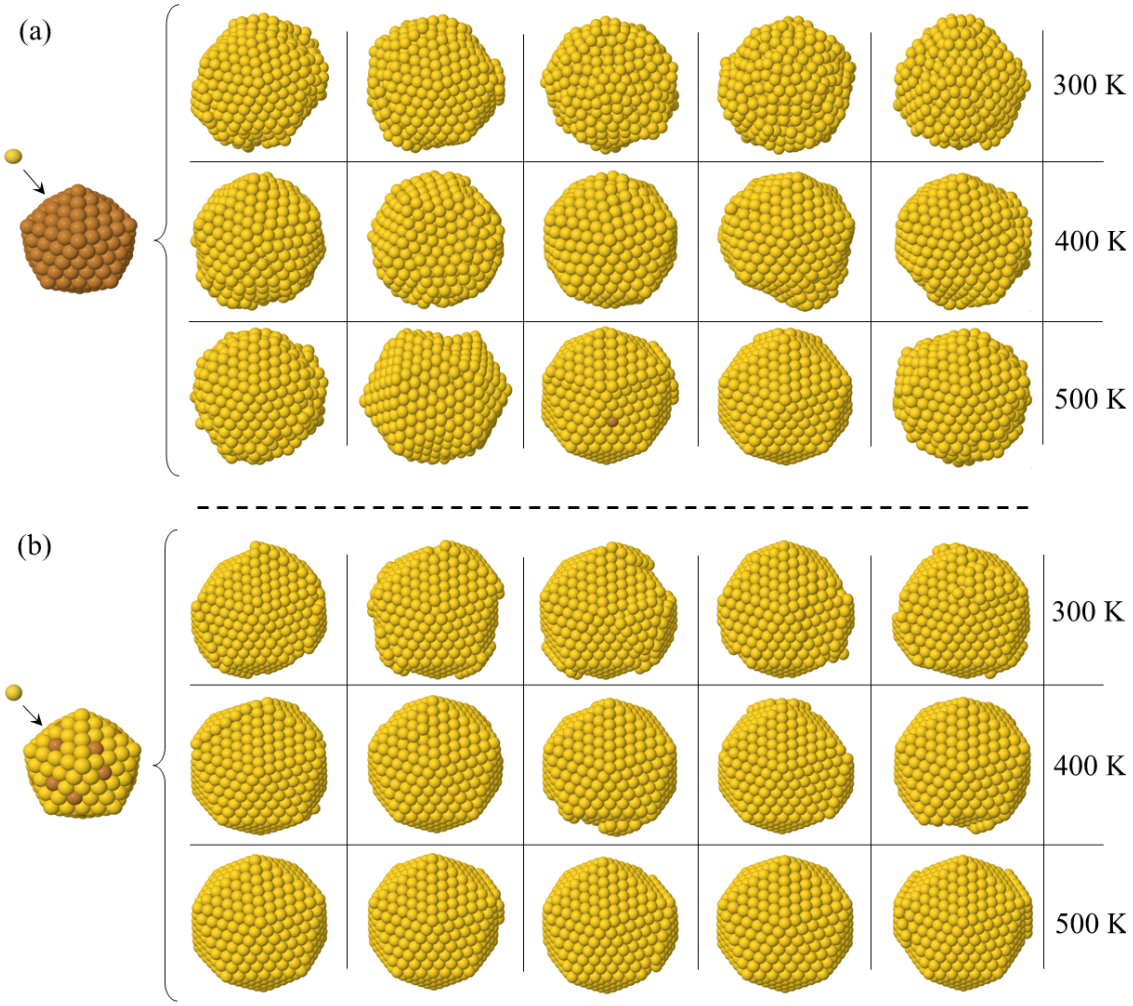

Figure S6: Surface view of the final structures obtained during the growth on Ih seeds with pure Cu (a) and intermixed CuAu (b) compositions. For each seed, we show the final structures of the five performed simulations at three different temperatures. The deposition of Au atoms every 10 ns on both Cu and CuAu Ih seeds leads to the formation of icosahedral motifs in all simulations. The surface of these Ih structures is anti-Mackay and rough in the case of Cu seed and it is Mackay and smooth in the case of CuAu seed.

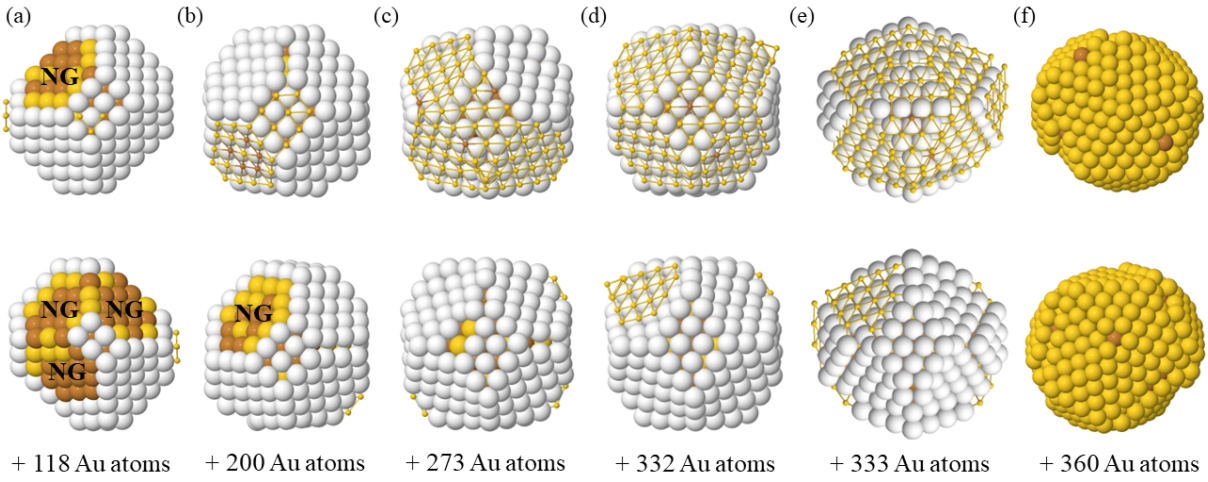

Figure S7: Growth pathway of icosahedral shape from TO copper seed obtained at temperature 500 K with deposition rate of 0.1/ns. For each size, the same structure is shown from two different perspectives. First formed layers on different facets of initial TO-201 shaped cluster are represented by withe atoms. Grids show the nucleation of a second layers on top of white ones. (a)-(b) formation of one layer-shell on the initial TO-201 shaped seed. (c)-(d) TO-405 where its squared-(100) facets are reconstructed to diamond ones. (e) transformation of the reconstructed TO-405 to an icosahedral shape. (f) defective icosahedron of size 561 atoms.

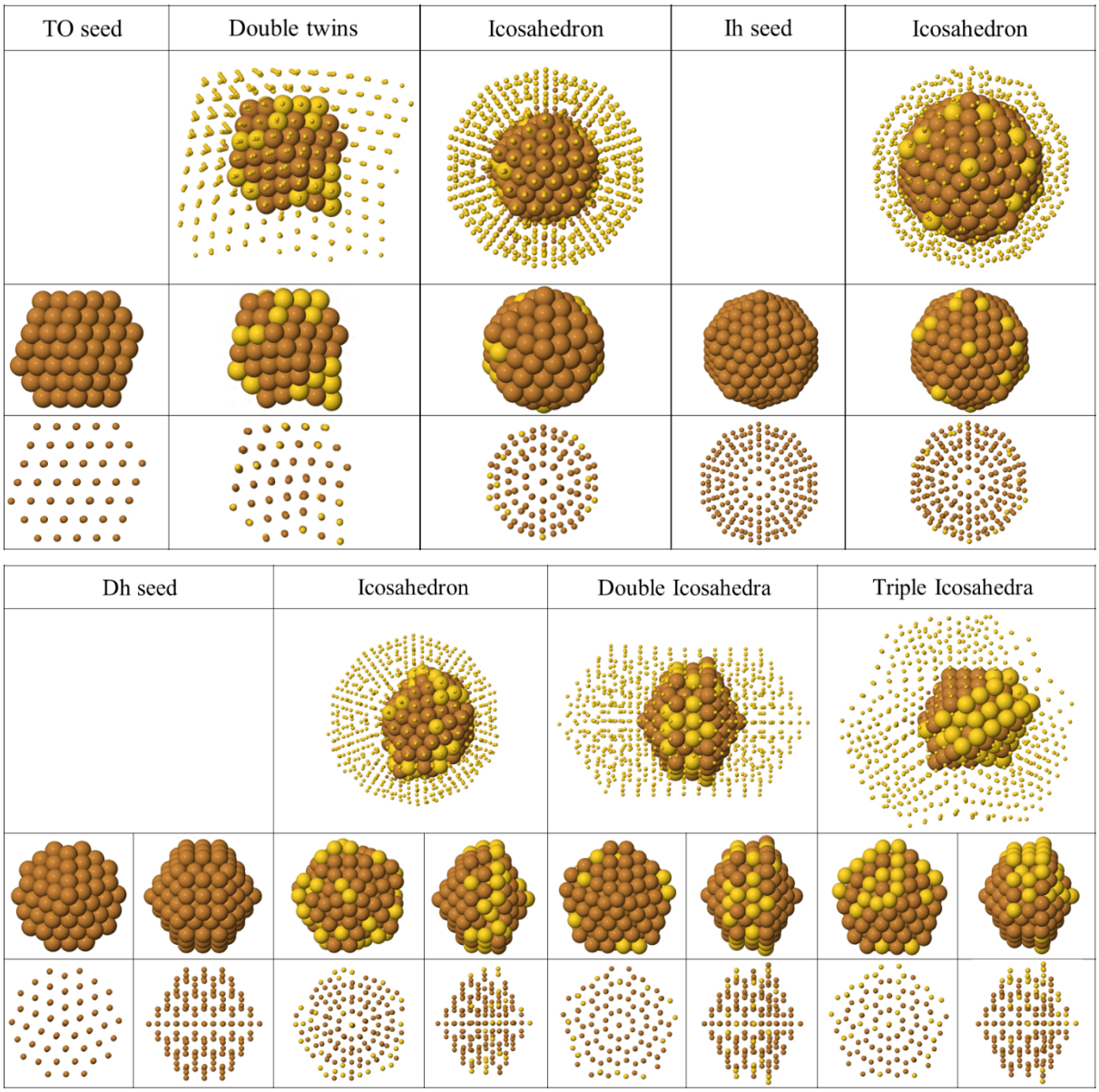

Figure S8: Exotic nanoparticles obtained during the growth on pure seeds. Surface views of these structures are shown in Fig. 2 in the main text. First table represents the core of the final exotic structures produced from the growth on TO and Ih seeds together with the starting TO and Ih seeds. Second table shows the core of the exotic structures achieved during the growth on Dh seed in comparison with the starting Dh seed.

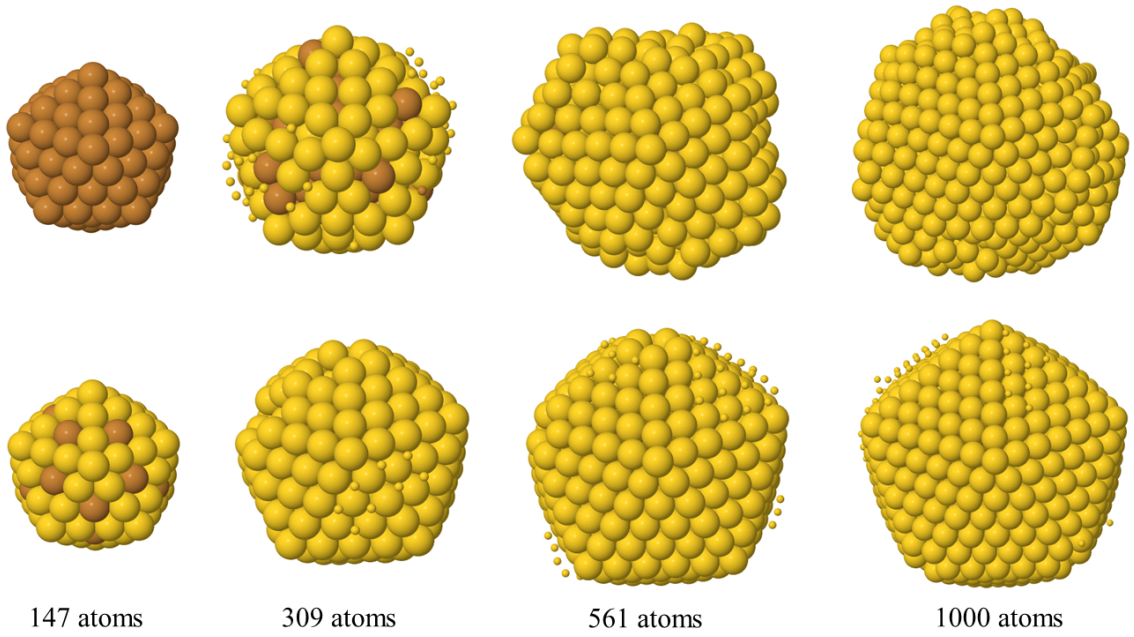

Figure S9: Snapshots from growth simulations at T=300 K and deposition rate of 1 atom/ns. The simulation is started from an icosahedron of 147 atoms, which grows to an irregular icosahedron in the case of the growth on pure seed and to regular icosahedron in the case of the growth on mixed seed.

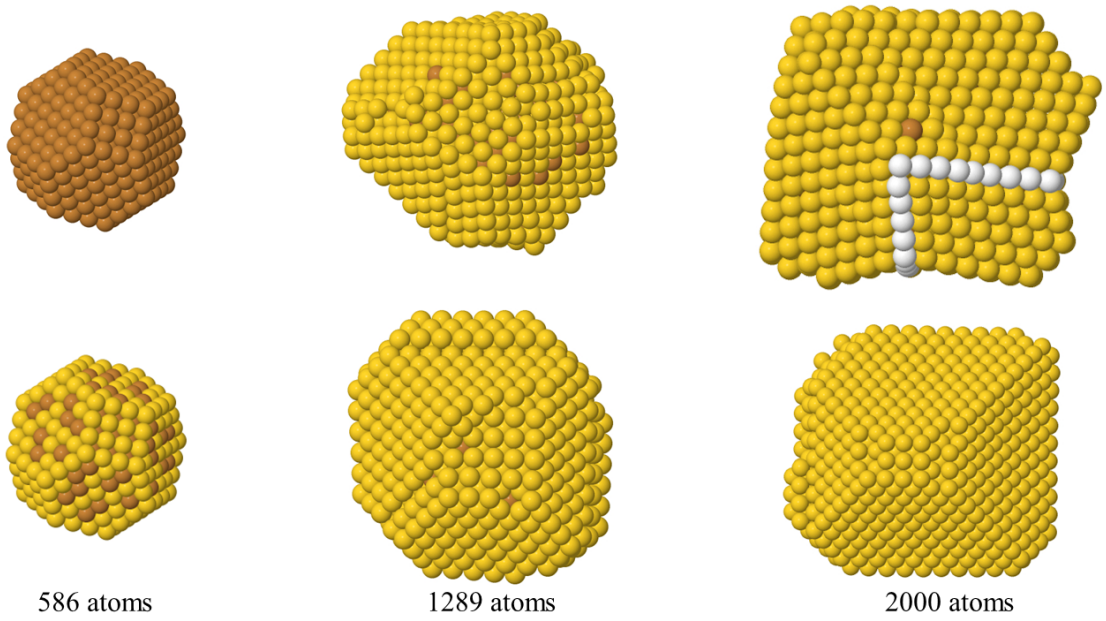

Figure S10: Snapshots from growth simulations at T=500 K and deposition rate of 1 atom/ns. The simulation is started from a truncated octahedron of 586 atoms, which grows to a double twin structure in the case of the growth on pure seed and to an octahedron in the case of the growth on mixed seed.